

Integrated synthesis of nanosized semiconductors in a bioremediation system for the treatment of AMD using biologically produced sulfide

João PINTO DA COSTA¹, Ana Violeta GIRÃO², João P. LOURENÇO³, Olinda C. MONTEIRO⁴,
Tito TRINDADE², Maria Clara COSTA^{1,*}

¹ Centro de Ciências do Mar, CCMar, Faculdade de Ciências e de Tecnologia, Campus de Gambelas, 8005–139 Faro, Portugal. ² Centro de Investigação em Materiais Cerâmicos e Compósitos, CICECO, Campus Universitário de Santiago, 3810–193 Aveiro, Portugal. ³ Centro de Investigação em Química do Algarve, CIQA, Faculdade de Ciências e de Tecnologia, Campus de Gambelas, 8005–139 Faro, Portugal ⁴ Centro de Química e Bioquímica, CQB, Faculdade de Ciências Universidade de Lisboa, Campo Grande 1749–016, Lisboa, Portugal.

*Corresponding author: mcorada@ualg.pt

Abstract The use of sulfate-reducing bacteria in bioremediation processes for the treatment of effluents with high-content of sulfate and metal generates an excess of sulfide. The elimination of this excess sulfide is a problem that needs to be addressed. Metal nano-sulfides, such as CuS and ZnS, have attracted much attention due to their excellent potential in catalysis, optical and electronic functionalities. In the present work, we set out to produce sulfide nanoparticles by combining a well-established bioremediation system into the synthesis process, thus allowing for an integrated environmentally friendly solution for some challenges facing the metallurgical and extractive industries.

Keywords nanoparticles, metal sulfides, bioremediation.

Introduction

Semiconductor nanocrystals possess unique optical and electronic properties, which bestow them with a huge potential in a wide range of applications (Sweeney *et al.* 2004). Of these, zinc sulfide (ZnS), copper sulfide (CuS) and iron sulfide (FeS) are of special interest. ZnS is photoconductive, luminescent and a piezoelectric material, making this compound suitable to be applied in solar cells, light emitting diodes, probes for the determination of proteins and photodegradation of organic compounds (Stanic *et al.* 1997; Yanagida *et al.* 1990; Zhu *et al.* 2004). CuS nanomaterials have a wide range of applications, which include catalysts (Liu and Xue 2009), nano-switches (Sakamoto *et al.* 2003), optical filters (Chen *et al.* 2009), solar radiation absorber (Li *et al.* 2009), among others. Iron sulfides are recognized as advanced inorganic materials with high potential in many applications, such as

high-density batteries, chalcogenide glasses and solar energy materials (Chin *et al.* 2005). The synthesis of all these nanomaterials has been described using a wide variety of methods, including the use of surfactants, organic solvent micro-emulsions, controlled double-jet precipitation, hydrothermal synthesis, liquid-solid phase synthesis, chemical vapor deposition, high gravity or gas phase decomposition, among others (Bessergenev *et al.* 1995; Biswas *et al.* 2007; Chen *et al.* 2004; Close *et al.* 1999; Ding *et al.* 2007; Thurston and Wilcoxon 1999; Xu and Zhang 2008). In general, these methods rely on the use of high temperatures, as well as high pressures, radiation and sometimes hazardous chemicals.

During sulfide-mining operations, sulfidic rock comes into contact with the surface or groundwater. Under oxidizing conditions, pyrite-containing rock produces sulfuric acid and dissolved iron. In turn, these acidic waters

then dissolve other metals contained in the rock, resulting in a low-pH, metal-bearing water known as acid mine drainage (AMD) or acid rock drainage (ARD; Doshi 2006). As a result, in some of those areas several mine lakes are very acidic ($\text{pH} < 3$) and contain high concentration of sulfate (up to 3.5 g/L) and metals, particularly iron, zinc and copper (Martins *et al.* 2008). Passive treatments, such as bioremediation using sulfate-reducing bacteria (SRB) have proven to be a good solution (Garcia *et al.* 2001; Huisman *et al.* 2006). Previously, work has been carried out in our group and a bioremediation system for AMD has been successfully developed (Martins *et al.* 2010). The selective precipitation of metals from multi-metal containing systems, such as wastewaters and soils, has been previously studied, using either chemical sulfide sources or biogenic sulfide (Fang *et al.* 2012; Sahinkaya *et al.* 2009; Sampaio *et al.* 2009; Tokuda *et al.* 2008). However, when reported, the particles obtained were always in the micron range ($>1 \mu\text{m}$). Previously, we have proven that the production of zinc sulfide nanoparticles ($<25 \text{nm}$) using SRB growth media containing biologically produced sulfide, at room temperature and atmospheric pressure, avoiding the use of additional and expensive chemicals, is a possibility (da Costa *et al.* 2012). Moreover, it has been demonstrated that the use of growth media of different complexities, as well as the filtration or not of these same media, yielded nanoparticles (NP's) with no considerable differences amongst one another. Using this previously acquired knowledge, we set out to, in the present work, selectively synthesize metallic (Cu^{2+} , Fe^{2+} and Zn^{2+}) sulfide nanoparticles. This was achieved using artificial metallic solutions as a source of the metal ions and real AMD in the feeding of the continuous bioremediation system, used as the source of sulfide, thus demonstrating the feasibility of this method of synthesis.

Materials and Methods

The bioremediation system used was the one

previously described by (Martins *et al.* 2010) and the synthesis principle has been described by (da Costa *et al.* 2012). After reaching continuous operation, the excess sulfide produced by the SRB in the bioremediation system was used as the sulfide source for the precipitation of the metals. The metal-containing solutions were prepared using distilled water and a combination of Cu^{2+} ($\text{CuSO}_4 \cdot 5\text{H}_2\text{O}$, $>99\%$, Riedel-Haën), Zn^{2+} ($\text{ZnSO}_4 \cdot 7\text{H}_2\text{O}$, $>99.5\%$, Panreac) and Fe^{2+} ($\text{FeSO}_4 \cdot 7\text{H}_2\text{O}$, $>99\%$, Panreac). These salts were added so that an approximate final concentration of $100 \text{mg} \cdot \text{L}^{-1}$ of each metal ion was obtained. The initial pH was corrected to 2.1, using a 6M solution of HNO_3 (Panreac). Sulfide concentration was measured immediately after sampling using a UV-visible spectrophotometer (DR2800 spectrometer, Hach-Lange) by the Methylene Blue Method (665 nm, Hach-Lange). The pH values were measured using a pH Meter (GLP 21, Crison) and corrected to 5.0 and 6.5 after the first and second precipitation steps, respectively, using a 2M NaOH solution, which was added drop-by-drop. Metal concentrations, before and after precipitation, were determined by flame atomic absorption spectroscopy using a Shimadzu AA-680 model spectrometer. XRD analyses were done using a PANalytical X'Pert Powder diffractometer with an X'Celerator detector, at 45 kV and 40 mA, with a step size (2θ) of 0.016. Transmission Electron Microscopy (TEM) coupled to EDX was carried out using a FEG-TEM Hitachi H9000 microscope operating at 300 kV. The samples were prepared by placing a drop, containing the precipitates dispersed in ultra-pure distilled water, on a copper grid coated with amorphous carbon film.

Results and Discussion

A solution containing $96 \text{mg} \cdot \text{L}^{-1}$ of copper, $103.7 \text{mg} \cdot \text{L}^{-1}$ of zinc and $104.04 \text{mg} \cdot \text{L}^{-1}$ of iron, at pH 2.1, was used. Fig. 1A shows the removal percentage, as well as each metal concentration after every precipitation step. Also shown are the removal efficiencies of all metals for the overall process. As observed, the first pre-

precipitation step seems to be very selective in the removal of copper, resulting in the precipitation of only minor amounts of zinc and iron. At the end of the second precipitation step (Fig. 1A), the remainder copper still in solution is, in essence, completely removed in all samples, never exceeding a concentration of 5 mg.L⁻¹. At this step, there is also an undesired high removal of iron (77%), and, at the last precipitation step, at which the removal of iron is desired, this is achieved in almost its entirety (>93% of the iron in solution after the second precipitation step). Overall, the process re-

moved 93 to 97% of all the metals present. The final pH, after all precipitation steps, ranged between 7.2–7.5. Having successfully removed the metals from the solutions, the precipitates obtained at each step were analyzed by X-ray diffraction (XRD) and the results obtained are shown in Fig. 1B. In the diffractogram of the first precipitate, the peaks corresponding to covellite (CuS, JCPD #00-001-1281) are clearly present, as well as in the other precipitates; however, in the second precipitate, peaks consistent to those corresponding to sphalerite (ZnS) are also present (JCPD #00-003-0579).

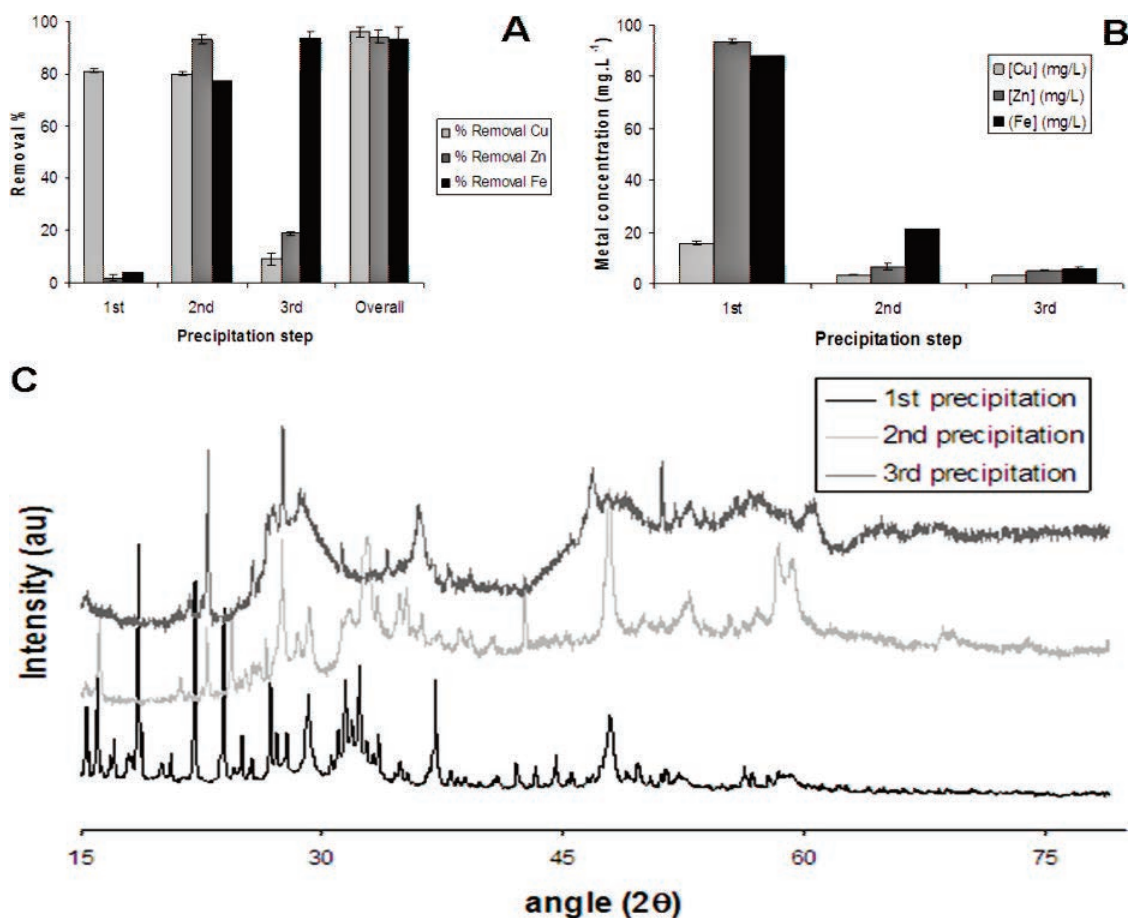


Fig. 1 In A, metal (Cu, Zn and Fe) removal percentages as well as the overall removal percentage for each metal at the end of the each precipitation step. In B, the concentrations of each metal at the end of each precipitation step. In both A and B, error bars are shown. In C, the X-ray diffractograms of the precipitates obtained at each step. Due to the high profusion of peaks, the identified phases are not indicated for simplification purposes. These, however, included covellite (CuS; JCPD #00-001-1281), sphalerite (ZnS; JCPD #00-003-0579) and iron (III) hydroxide (JCPD #00-038-0032).

These also contribute to the diffractogram of the precipitate obtained at the third precipitation step, in which peaks corresponding to iron (III) hydroxide are visible (JCPD #00-038-0032). Overall, these results corroborate those illustrated in Figs. 1A and 1B, further indicating that the precipitation process that herein described is very selective for copper and less discriminatory when precipitating zinc and iron. Also, in the case of the latter metal, it should be noted that the corresponding crystallites identified were hydroxides, not sulfide. This may be due to the fact that the addition of the NaOH for the correction of the pH may culminate in the formation of the iron hydroxide.

The elemental and morphological characterization was done by TEM-EDX. In Fig. 2, the TEM images obtained for each precipitate synthesized at each precipitation step are shown (Fig. 2A – 2C). The corresponding EDX spectra

are shown in Figs. 2D – 2F. The precipitates all seem to show spheroid morphology, with sizes ranging between 20 – 30 nm, though some needle-like structures are identifiable in the precipitate obtained at the third step. The EDX results are consistent with the removal efficiency data, shown in Fig. 1. The main precipitated phase, in the first precipitation step, is CuS, with traces of both Fe and Zn.

This highlights the high selectivity of this method for precipitating CuS, with minimal co-precipitation of Zn and Fe species. At the second precipitation step, ZnS is the main phase present, followed by FeS and, to a smaller extent, CuS. The former is the main phase present in the precipitate obtained at the final step. However, ZnS is also present, as well as some amounts of Cu. Nonetheless, it should be noted that the presence of copper in other precipitates other than the one ob-

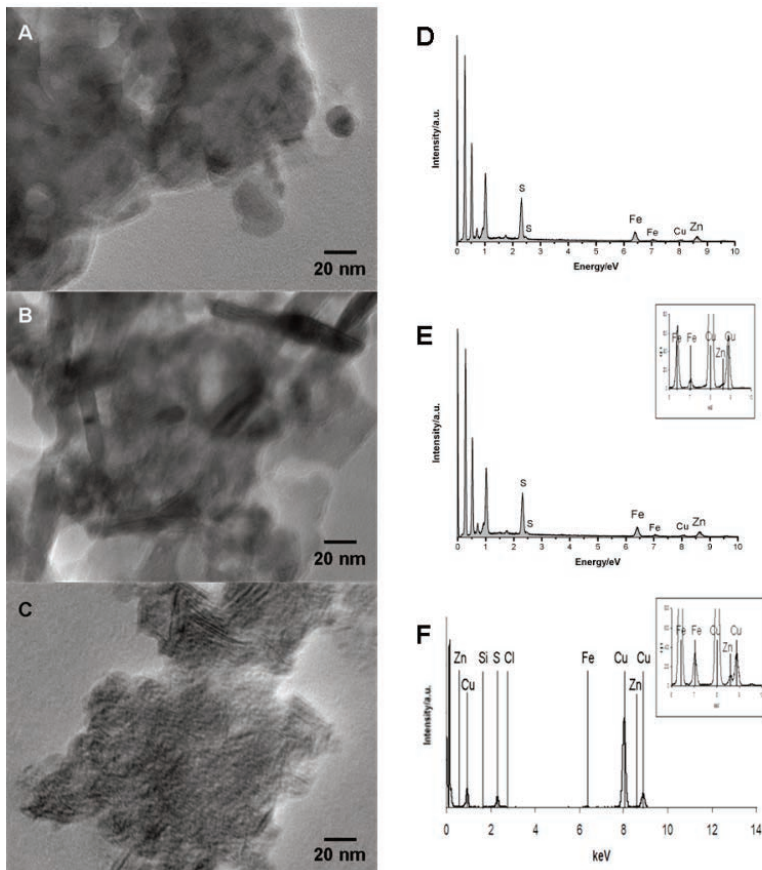


Fig. 2 TEM images of the precipitates obtained at steps 1, 2 and 3 (A, B and C, respectively). Also shown are the corresponding EDX analyses (2D – 2F). The elements identified are shown. Due to the composition of the grid (Cu) and the high relative presence of this element, insets are shown, evidencing the presence or absence of Fe as well as of Zn in the precipitates obtained at the second and third steps.

tained initially should be carefully discussed, as the TEM grid used is composed of copper. Consequently, this element appears prominent in the analyses made for the precipitates obtained at the end of both the second and third steps. Additionally, Cl was also found, which is not surprising, considering that the water used for the preparation of the growth media is tap water. Interestingly, traces of Si were also identified in the last sample, which may result from either cross-contamination with other samples (in which SiO₂ was used) or from the fact that this sample was kept in a glass vial.

Conclusions and Future Perspectives

In summary, by integrating a previously described bioremediation system and a synthesis process for obtaining nano-sized metal sulfides, we were able to selectively precipitate CuS nanoparticles and ZnS particles, though the latter with a smaller degree of selectivity. The precipitation of FeS was not achieved, with the Fe precipitates consisting, mostly, of hydroxides (Fig. 1B). The authors speculate that this limitation, however, may be circumvented by using, for example, on-line systems for the accurate control of pH. Moreover, the implementation of a completely oxygen-free environment may contribute for obtaining Fe precipitates in the form of sulfides, thus resulting in a final highly selective recovery process of metal sulfides. Finally, the use of real metal-containing wastewaters, such as Acid Mine Drainage, may be a possibility, further contributing to an integrated green process, resulting in the simultaneous remediation of contaminated waters and concomitant metal sulfide nanocrystals production.

Acknowledgements

Funding by Fundação para a Ciência e a Tecnologia (FCT) through a PhD grant (SFRH/BD/43784/2008) and through project PTDC/AAG-TEC/2721/2012 is acknowledged. A. V. Girão also thanks FCT for the Post-Doc grant (SFRH/BPD/66407/2009).

References

- Bessergenev V, Ivanova EN, Kovalevskaya YA, Gromilov SA, Kirichenko VN, Zemskova SM, Vasilieva IG, Ayupov BM, Shwarz NL (1995) Optical and Structural Proper Ties of ZnS and ZnS-Mn Films Prepared by Cvd Method. *Mater Res Bull* 30(11): 1393-1400.
- Biswas S, Kar S, Chaudhuri S (2007) Thioglycolic acid (TGA) assisted hydrothermal synthesis of SnS nanorods and nanosheets. *Appl Surf Sci* 253(23): 9259-9266.
- Chen JF, Li YL, Wang YH, Yun J, Cao DP (2004) Preparation and characterization of zinc sulfide nanoparticles under high-gravity environment. *Mater Res Bull* 39(2): 185-194.
- Chen LF, Yu W, Li Y (2009) Synthesis and characterization of tubular CuS with flower-like wall from a low temperature hydrothermal route. *Powder Technol* 191(1-2): 52-54.
- Chin PP, Ding J, Yi JB, Liu BH (2005) Synthesis of FeS₂ and FeS nanoparticles by high-energy mechanical milling and mechanochemical processing. *J Alloy Compd* 390(1-2): 255-260.
- Close MR, Petersen JL, Kugler EL (1999) Synthesis and characterization of nanoscale molybdenum sulfide catalysts by controlled gas phase decomposition of Mo(CO)(6) and H₂S. *Inorg Chem* 38(7): 1535-1542.
- da Costa JP, Girao AV, Lourenco JP, Monteiro OC, Trindade T, Costa MC (2012) Synthesis of nanocrystalline ZnS using biologically generated sulfide. *Hydrometallurgy* 117: 57-63.
- Ding Y, Liu X, Guo R (2007) Synthesis of hollow PbS nanospheres in pluronic F127/cyclohexane/H₂O microemulsions. *Colloid Surface A* 296(1-3): 8-18.
- Doshi SM (2006) Bioremediation of Acid Mine Drainage Using Sulfate-Reducing Bacteria. U.S. Environmental Protection Agency, Office of Solid Waste and Emergency Response and Office of Superfund Remediation and Technology Innovation 65.
- Fang D, Zhang R, Liu X, Zhou L (2012) Selective recovery of soil-borne metal contaminants through integrated solubilization by biogenic sulfuric acid and precipitation by biogenic sulfide. *Journal of Hazardous Materials* 219-220(o): 119-126.
- Garcia C, Moreno DA, Ballester A, Blazquez ML, Gonzalez F (2001) Bioremediation of an industrial acid mine water by metal-tolerant sulphate-reducing bacteria. *Minerals Engineering* 14(9): 997-1008.

- Huisman JL, Schouten G, Schultz C (2006) Biologically produced sulphide for purification of process streams, effluent treatment and recovery of metals in the metal and mining industry. *Hydrometallurgy* 83(1-4): 106-113.
- Li F, Kong T, Bi WT, Li DC, Li Z, Huang XT (2009) Synthesis and optical properties of CuS nanoplate-based architectures by a solvothermal method. *Appl Surf Sci* 255(12): 6285-6289.
- Liu J, Xue DF (2009) Solvothermal synthesis of CuS semiconductor hollow spheres based on a bubble template route. *J Cryst Growth* 311(3): 500-503.
- Martins M, Santos ES, Pires C, Barros RJ, Costa MC (2010) Production of irrigation water from bioremediation of acid mine drainage: comparing the performance of two representative systems. *J Clean Prod* 18(3): 248-253.
- Martins MSF, Santos ES, Barros RJ, Costa MCSD (2008) Treatment of Acid Mine Drainage with Sulphate-reducing Bacteria Using a Two-stage Bioremediation Process. *Mine Water and the Environment Proceedings*: 297-300
- Sahinkaya E, Gungor M, Bayrakdar A, Yucesoy Z, Uyanik S (2009) Separate recovery of copper and zinc from acid mine drainage using biogenic sulfide. *Journal of Hazardous Materials* 171(1-3): 901-906.
- Sakamoto T, Sunamura H, Kawaura H, Hasegawa T, Nakayama T, Aono M (2003) Nanometer-scale switches using copper sulfide. *Appl Phys Lett* 82(18): 3032-3034.
- Sampaio RMM, Timmers RA, Xu Y, Keesman KJ, Lens PNL (2009) Selective precipitation of Cu from Zn in a pS controlled continuously stirred tank reactor. *Journal of Hazardous Materials* 165(1-3): 256-265.
- Stanic V, Etsell TH, Pierre AC, Mikula RJ (1997) Sol-gel processing of ZnS. *Mater Lett* 31(1-2): 35-38.
- Sweeney RY, Mao CB, Gao XX, Burt JL, Belcher AM, Georgiou G, Iverson BL (2004) Bacterial biosynthesis of cadmium sulfide nanocrystals. *Chem Biol* 11(11): 1553-1559.
- Thurston TR, Wilcoxon JP (1999) Photooxidation of organic chemicals catalyzed by nanoscale MoS₂. *Journal of Physical Chemistry B* 103(1): 11-17.
- Tokuda H, Kuchar D, Mihara N, Kubota M, Matsuda H, Fukuta T (2008) Study on reaction kinetics and selective precipitation of Cu, Zn, Ni and Sn with H(2)S in single-metal and multi-metal systems. *Chemosphere* 73(9): 1448-1452.
- Xu ZY, Zhang YC (2008) In air liquid-solid phase synthesis of metal sulfide nanoparticles from metal acetates and thiourea. *Mater Chem Phys* 112(2): 333-336.
- Yanagida S, Yoshiya M, Shiragami T, Pac CJ, Mori H, Fujita H (1990) Semiconductor Photocatalysis .9. Quantitative Photoreduction of Aliphatic-Ketones to Alcohols Using Defect-Free ZnS Quantum Crystallites. *J Phys Chem-US* 94(7): 3104-3111.
- Zhu CQ, Zhao DH, Chen JL, Li YX, Wang Y, Wang L, Zhou YY, Zhuo SJ, Wu YQ (2004) Application of L-cysteine-capped nano-ZnS as a fluorescence probe for the determination of proteins. *Anal Bioanal Chem* 378(3): 811-5.